2022 IEEE 25th International Conference on Intelligent Transportation Systems (ITSC)
October 8-12, 2022, Macau, China

Integrated control of traffic signal and automated vehicles for mixed traffic: Platoon-based bi-level optimization approach

Yangang Zou, Fangfang Zheng, Zhichen Fan, Youhua Tang

2022 IEEE 25th International Conference on Intelligent Transportation Systems (ITSC) | 978-1-6654-6880-0/22/$31.00 ©2022 IEEE | DOI: 10.1109/ITSC55140.2022.9922535

***Abstract*—Connected and autonomous vehicle (CAV) technologies are widely recognized to help improve the operational efficiency of urban road traffic systems and thus mitigate traffic congestion. In this study, we propose a bi-level integrated control method to optimize traffic signals and automated vehicle trajectories simultaneously for mixed traffic with human-driven vehicles (HDVs) and CAVs. Instead of considering individual vehicles in the optimization process, the vehicles are divided into platoons, which are used as the basic units for optimal control, such that the computational cost can be reduced. A mixed integer linear programming (MILP) model is developed to optimize the signal timing scheme and arrival time of the platoon at the stop line with the objective of minimizing the total delay. Based on the optimized arrival time, the trajectory of the first CAV in the moving platoon is optimized to reduce the start-stop phenomenon at the intersection. Numerical experiments are performed and the results demonstrate that the proposed method outperforms the vehicle-actuated control method significantly in terms of the delay and fuel consumption reduction under different traffic conditions. Furthermore, the performance improvement of the proposed model compared to that of the vehicle-actuated control method increases substantially with the increase of the CAV penetration rate.**

I. Introduction

In the urban road network, intersections are considered as the main bottlenecks, which have significant impacts on safety and efficiency of traffic operations. In recent years, the rapid development of connected and autonomous vehicle (CAV) technologies provides the opportunity to better manage and control intersection operations to improve safety and reduce traffic congestion.

The study on signal control using CAV technologies can be categorized as: signal control only, optimal control of vehicle trajectories, and joint control of traffic signals and vehicle trajectories. Signal control algorithms focus on optimizing signal timings and phase sequences based on massive CAV data with the objective of maximizing traffic efficiency. The vehicle trajectory optimization control mainly adjusts vehicle trajectories by informing the vehicle signal phase and timing (SPaT) and surrounding vehicle information, aiming to improve fuel economy (or reduce vehicle emissions) [1-5], reduce travel time [1, 4], improve comfort [4], and increase intersection capacity [6]. However, these studies do not take full advantages of V2I communication because they do not consider signal optimization [7]. Compared with the above discussed control categories, the joint control of traffic signals and vehicle trajectories can maximize the potential of CAV technologies. The signal control and vehicle trajectory control are actually interdependent: the signal timing affects the motion of individual vehicles and thus their performance (e.g., emissions and fuel consumption), while vehicle trajectories are the key inputs of traffic control models [8]. This interdependence is usually modeled using a bi-level optimization framework [9-12].

Most of the above studies consider scenarios where the CV/CAV penetration rate is 100%. However, the realization of such scenarios is still decades away in reality [13]. Therefore, investigating the mixed traffic system, wherein both HDVs and CAVs coexist, is of more practical significance. For the mixed traffic scenario, traffic states including the positions (or speeds) of HDVs [14, 15], queue length[16], or travel time [17] can be estimated using the information obtained by CAVs. Based on the estimated state information, the traffic signal scheme can be optimized using the enumeration method [9, 10, 12] or dynamic programming approach [11, 14, 18-21]. Owing to the increasing complexity of research scenarios and higher requirement of control accuracy, the mixed integer linear programming (MILP) method is applied to model traffic operations at intersections and some existing solvers are used to solve the optimization problem [7, 10, 22]. However, the large computational effort makes it difficult to obtain timely optimization results for these methods, and thus limits their practical applications.

To reduce the model complexity and computational burden, it is preferable to consider the platoon in which vehicles have the similar motion state as the basic optimization unit. For example, Yu et al.[23] optimize vehicle trajectories and traffic signals in a unified framework at an isolated urban intersection with expectation of reducing vehicle delays and emissions. In their study, vehicles that pass a stop bar in the same lane within the same cycle are regarded as one platoon. Unlike the platoon division strategy of Yu et al. [23], Feng et al. [11] divide the platoon and estimate the platoon size based on the vehicle distance and traffic state.

This work was funded by National Natural Science Foundation of China (NSFC) under grant 52072315, National Key R&D Program of China under grant 2021YFB1600100, and Department of Science & Technology of Sichuan Province under project codes 2020JDJQ0034 and 2022YFG0152.

Y. Zou is with School of Transportation and Logistics, Southwest Jiaotong University, 611756, P.R. China (e-mail: yangang.zou@my.swjtu.edu.cn).

F. Zheng is with School of Transportation and Logistics, National Engineering Laboratory of Integrated Transportation Big Data Application Technology, National United Engineering Laboratory of Integrated and Intelligent Transportation, Southwest Jiaotong University, 611756, P.R. China (Corresponding author, e-mail: fzheng@swjtu.cn).

Z. Fan is with School of Transportation and Logistics, Southwest Jiaotong University, 611756, P.R. China (e-mail: fzc@swjtu.edu.cn).

Y. Tang is with School of Transportation and Logistics, National Engineering Laboratory of Integrated Transportation Big Data Application Technology, National United Engineering Laboratory of Integrated and Intelligent Transportation, Southwest Jiaotong University, 611756, P.R. China (e-mail: tyhctt@swjtu.cn).

They further propose a bi-level optimization framework, wherein the first level optimizes the signal timing modeled as a dynamic programming (DP) problem with the objective of minimizing vehicle delays, and the second layer optimizes vehicle trajectories with the goal of minimizing fuel consumption and emissions. However, both of above studies are only applicable to 100% CAV traffic.

To the best of our knowledge, the research on integrated optimization of signals and vehicle trajectories in the mixed traffic environment is rather limited. Though Liang et al. [24] propose an integrated optimization approach to jointly optimize the signal timing scheme and the CAV trajectory. The focus is on the comparison of computational efficiency between their proposed platoon-based model and the individual vehicle-based control method. The effectiveness of their method (e.g., in terms of delay, fuel consumptions) needs to be further investigated.

In this study, we propose a bi-level optimization framework for the integrated optimization of traffic signals and vehicle trajectories at the isolated intersection in the mixed traffic environment. The vehicles are divided into platoons based on the information collected from CAVs within the communication zone of the intersection. The upper level is a MILP model with the objective of minimizing vehicle delays. The signal timing scheme and arrival time of the platoon at the stop line are optimized. The lower level optimizes the trajectory of the first CAV in the moving platoon based on the planned arrival time obtained from the upper level to reduce the total number of vehicle stops. Simulation experiments are used to validate the effectiveness of the proposed approach.

II. PROBLEM DESCRIPTION

This study considers the scenario of a road section with an isolated intersection controlled by the traffic signal, where the mixed traffic streams of HDVs and CAVs are traveling on the road as shown in Fig. 1. Both CAVs and signal control are equipped with V2V/V2I communication devices (e.g., DSRC, LTE-V or 5G). The information of CAVs (e.g., position, speed, and acceleration/deceleration) within the communication range (e.g., 300m) can be obtained and used to identify different platoons, and further to estimate the number of vehicles in the platoon.

Fig. 2 shows the proposed bi-level optimization framework which combines traffic signal optimization with the CAV trajectory planning in the mixed traffic flow. The upper level optimizes the signal timing and desired arrival time of the platoon based on the estimated platoon size with the objective of minimizing the total delay. The lower level optimizes the trajectory of the first CAV in each platoon based on the desired arrival time to reduce the start-stop phenomenon of vehicles at intersections, while the HDVs within the platoon are assumed to be in the following state described by the car-following model.

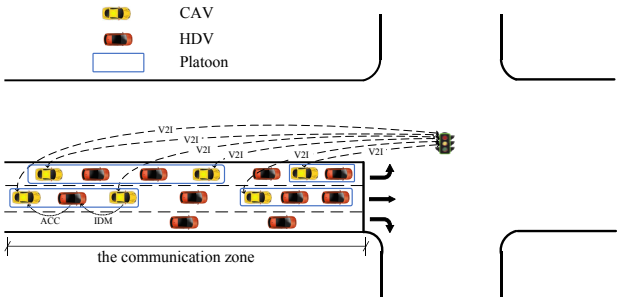

Figure 1. Platoon identification under the mixed traffic environment.

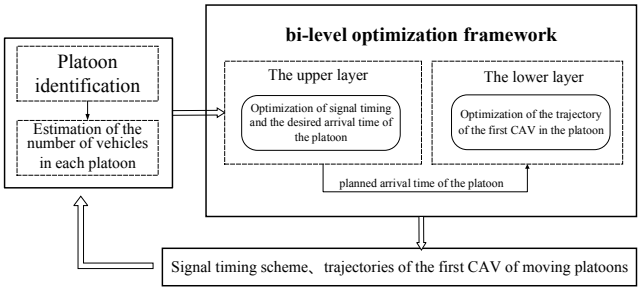

Figure 2. Bi-level integrated optimization control framework.

III. PLATOON IDENTIFICATION AND ESTIMATION

A. Platoon identification

To facilitate the integrated optimization process and reduce computational costs, we consider the platoon as the basic optimization unit in the integrated optimization. Fig.3 shows the platoon division when approaching the intersection, wherein the stationary queuing CAVs are grouped into a single platoon, and the moving CAVs are divided into different platoons based on the headway spacing.

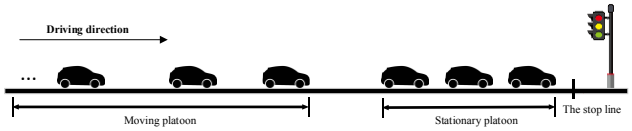

Figure 3. Two types of platoons near the intersection

We denote the critical headway spacing between the two adjacent CAVs (with 100% CAV penetration rate) in the steady state as X_1 , then the critical headway spacing X_p at the CAV penetration rate $P(0 < P \le 1)$ can be estimated according to the method of calculating the critical headway proposed by He et al.[25] as given by

$$X_p = \frac{X_1}{P} \tag{1}$$

If the headway spacing between the two adjacent CAVs Δx is less than or equal to $X_P(\Delta x \le X_P)$, these two CAVs are considered in the same platoon; otherwise, they are in different platoons. The detailed platoon identification procedure is shown in Fig.4.

It is worth noting that a platoon may consist of only one CAV. This can occur when the traffic volume is very low, or the CAV penetration rate is low or only one CAV is traveling

in a group of moving HDVs. Even though the platoon consists of only one CAV, it is still worthwhile to perform the CAV trajectory planning and control, which could have an impact on the undetected HDVs following this CAV.

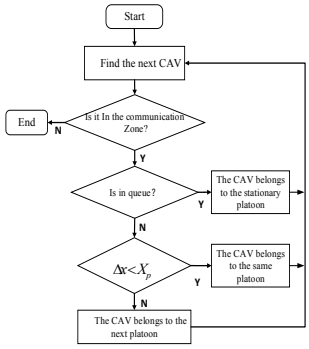

Figure 4. Platoon identification process

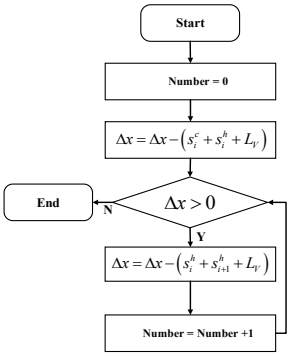

Figure 5. Estimation of the number of vehicles between two adjacent CAVs

B. *Estimation of the platoon size*

For the stationary platoon, we assume that the queueing headway spacing of the CAVs and HDVs is the same. The number of vehicles N_q can be estimated as

$$N_q = \frac{x_{last}}{s_q} \tag{2}$$

where x_{last} is the distance between the position of the last CAV and stop line. s_q is the queueing headway spacing.

For the moving platoon, we assume that all vehicles in the platoon travel with the same speed and all vehicles except the first (CAV) vehicle are in the car-following state. The number of vehicles in the platoon is estimated from the last vehicle in the platoon forward. Whether there is an HDV or there are more HDVs between two CAVs can be judged according to

$$\Delta x > s_i^c + s_i^h - L_v \tag{3}$$

$$\Delta x_i > s_i^h + s_{i+1}^h - L_v \tag{4}$$

where Δx is the gap distance between two adjacent CAVs as shown in Fig. 6 (a). Δx_i is the gap distance between the first CAV and inserted HDV i as shown in Fig. 6. L_v is the average length of the vehicle. s_i^c represents the maximum of the safe headway spacing of CAV i and queueing headway spacing s_q, and s_i^h represents the maximum of the safe headway spacing of HDV i and queueing headway spacing, which can be calculated as

$$\begin{aligned} s_i^c &= \max(T_s^c v_i^c, s_q) \\ s_i^h &= \max(T_s^h v_i^h, s_q) \end{aligned} \tag{5}$$

where T_s^c and T_s^h represent the safe time headways of the CAV and HDV, respectively. v_i^c and v_i^h represent the speeds of CAV i and HDV i. Equation(3) indicates that if the gap distance between the two adjacent CAVs is much larger than the sum of the gap spacings of the CAV and HDV, as well as the length of the HDV, we assume that there is an HDV between these two adjacent CAVs, as shown in Fig. 6(a). If Equation (4) is satisfied, another HDV can be inserted in the platoon, as shown in Fig. 6(b). This step is repeated until Equation (4) is unsatisfied. In this way, we can estimate the number of vehicles in the moving platoon. The detailed estimation procedure of the number of vehicles between two adjacent CAVs is shown in Fig.5.

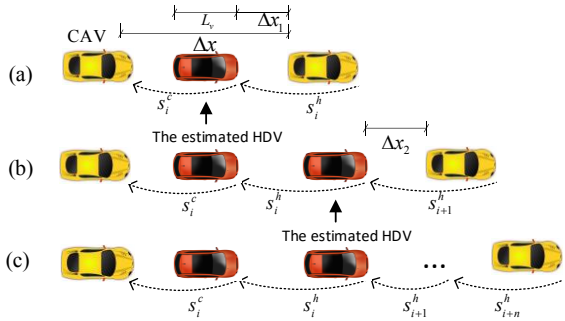

Figure 6. Illustration of the procedure to estimate the number of vehicles between two adjacent CAVs

IV. INTEGRATED OPTIMIZATION MODEL FORMULATION

A. *Model assumptions*

To make our research problem more concise and clear, we make the following assumptions.

1) The arrival of vehicles at the intersection follows the Poisson distribution, which is a common practice for traffic control at isolated intersections [23].

2) Vehicles complete the lane changes and overtaking before entering the communication zone of the intersection, and thus the lane change is not allowed in the communication zone of the intersection.

3) The time delay due to the information transmission and computation is not considered.

B. *Objective function*

We choose the total vehicle delay as the optimization objective for the proposed model. To simplify the calculation, the delay of each platoon is assumed to be the product of the delay of the first vehicle in the platoon and the number of vehicles in the platoon. The delay of the first vehicle is the difference between the planned time to leave the stop line and the free-flow arrival time at the stop line. In addition, it is possible that the total delay is the same for multiple optimization results with different cycle times. Thus, the minimization of the cycle time is used as a secondary objective to make the phasing more flexible. The objective function is formulated as

$$\min \alpha_1 \sum_y \sum_k N_{y,k} \left(t_{y,k}^L - t_c - \frac{L_{y,k}}{V_f} \right) + \alpha_2 \sum_j \sum_i g_{j,i} \tag{6}$$

where $N_{y,k}$ is the number of vehicles in the k^{th} platoon in lane y. $t_{y,k}^L$ is the moment when the first vehicle in the

k^{th} platoon in lane y leaves the stop line. t_c is the current time. $L_{y,k}$ is the distance from the first vehicle in the k^{th} platoon in lane y to the stop line to the stop line. V_f is the free-flow speed and $g_{j,i}$ is the green time of phase i in the j^{th} cycle. α_1, α_2 are the weight parameters.

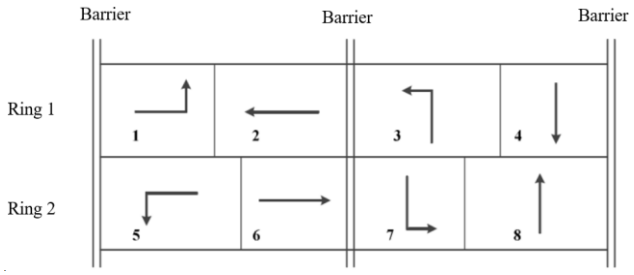

Figure 7. NEMA phase structure.

C. Phase structure constraints

The optimization model is based on a standard NEMA ring barrier signal structure as shown in Fig.7. No signal control is performed for the right turning vehicles.

The phase formulation is given by (7) - (13). It is worth noting that the signal optimization model can be built regardless of the current phase. We assume that the initial phase (1 and 5) is used for each signal cycle, which needs to be initialized by (7) and (8). Equations (9) - (11) represent the phase order in the NEMA double-ring signal structure. Equation (12) indicates that phases 2 and 6, and phases 4 and 8 need to end at the same time to meet the barrier condition. The duration of a phase is equal to the sum of the green time, yellow time and all-red clearance time as given by (13).

$$t_{1,1} = O_1 \tag{7}$$

$$t_{1,5} = O_2 \tag{8}$$

$$t_{j,2} = t_{j,1} + q_{j,1}, t_{j,3} = t_{j,2} + q_{j,2}, t_{j,4} = t_{j,3} + q_{j,3}, \forall j \tag{9}$$

$$t_{j,6} = t_{j,5} + q_{j,5}, t_{j,7} = t_{j,6} + q_{j,6}, t_{j,8} = t_{j,7} + q_{j,7}, \forall j \tag{10}$$

$$t_{j+1,1} = t_{j,4} + q_{j,4}, t_{j+1,5} = t_{j,8} + q_{j,8}, \forall j \tag{11}$$

$$q_{j,1} + q_{j,2} = q_{j,5} + q_{j,6}, q_{j,3} + q_{j,4} = q_{j,7} + q_{j,8}, \forall j \tag{12}$$

$$q_{j,i} = g_{j,i} + Y + R, \forall j, i \tag{13}$$

where O_1 is the start time of ring 1 and O_2 is the start time of ring 2. $t_{j,i}$ is the green start time of phase i in the j^{th} cycle. $q_{j,i}$ is the duration of phase i in the j^{th} cycle. Y is the yellow time and R is the all-red clearance time.

D. Green start time constraints

We denote the set of phases that has been executed and the set of current phases as Δ_p and Δ_c, respectively, and their green start times are given by (14) and (15). Equation (16) indicates that the green start time of the phase that has not been executed is greater than the current time.

$$t_{j,i} = t_{j,i}^p \forall (j,i) \in \Delta_p \tag{14}$$

$$t_{j,i} = t_{j,i}^o \forall (j,i) \in \Delta_c \tag{15}$$

$$t_c \le t_{j,i} \forall (j,i) \in \Delta - \Delta_p - \Delta_c \tag{16}$$

where $t_{j,i}^p$ is the green start time of phase i in the j^{th} cycle in set Δ_p. $t_{j,i}^o$ is the green start time of phase i in the j^{th} cycle in set Δ_c, and Δ is the set of all phases.

E. Green duration constraints

Equation (17) provides the constraint for the green time which should fall between the minimum green time and maximum green time. For the phase that has been executed, the green time is specified by (18). In addition, Equation (19) indicates that the green time of the current phase needs to be greater than the green time that has been executed.

$$g_{\min} \le g_{j,i} \le g_{\max} \ \forall (j,i) \in \Delta \tag{17}$$

$$g_{j,i} = g_{j,i}^p \ \forall (j,i) \in \Delta_p \tag{18}$$

$$g_{j,i} \ge t_c - t_{j,i}^o \ \forall (j,i) \in \Delta c \tag{19}$$

where $g_{j,i}^p$ is the green duration of phase i in the j^{th} cycle in set Δ_p. $g_{\min}$ is the minimum green time and $g_{\max}$ is the maximum green time.

F. Planning scope constraints

The number of planning cycles needs to be large enough to allow all platoons to pass through the intersection within the planning scope. A small j may make the model infeasible, and a large j will increase the computational burden of the model. We use the method proposed in [23] to determine the value of j. The basic idea is that first we let $j = 1$ and determine whether there is a feasible solution for the model. If not, we update $j = j + 1$ until a feasible solution is found.

G. Platoon selection through phase constraints

To ensure each platoon passes through the intersection completely within one cycle, the sum of the arrival time of the platoon and the clearance time of the platoon should be less than the sum of the phase green start time and the green duration as given by

$$t_{y,k}^L + t_{y,k}^c \le t_{j,i} + g_{j,i} + M(1 - \theta_{y,k,j}), \forall y, k, j, i \tag{20}$$

In addition, the platoon can only choose one cycle to pass as given by

$$\sum_j \theta_{y,k,j} = 1, \ \forall y, k, j \tag{21}$$

where $t_{y,k}^L$ is the moment when the first vehicle in the k^{th} platoon in lane y leaves the stop line. $t_{y,k}^c$ is the clearance time of the k^{th} platoon in lane y. M is a sufficiently large number. $\theta_{y,k,j}$ is a binary variable with the following properties.

$$\theta_{y,k,j}=\begin{cases}1, & \text{if } platoon(y,k) \text{ passes through the intersection in cycle } j\\ 0, & \text{otherwise}\end{cases} \quad (22)$$

H. Platoon arrival time constraints

For a platoon that has reached the stop line and is at a standstill, the arrival time is set to be the same as the current moment as given by

$$t_{y,k}^{a}=t_c \ \forall(y,k)\in\Gamma_q \quad (23)$$

where Γ_q is the set of all stationary platoons. $t_{y,k}^{a}$ is the moment when the first vehicle in the k^{th} platoon in lane y arrives at the stop line.

For moving platoons, the arrival time of the platoon should satisfy the following constraint as given by

$$t_{y,k}^{a}\geq t_{y,k}^{f}+t_c \ \forall(y,k)\in\Gamma_m \quad (24)$$

where Γ_m is the set of all moving platoons. $t_{y,k}^{f}$ is the earliest time required for the platoon to arrive at the stop line, and it depends on the distance from the current position of the first vehicle of the platoon to the stop line, as given by

$$t_{y,k}^{f}=\begin{cases}\dfrac{V_f-v_{y,k}}{a_{\max}}+\dfrac{L_{y,k}-\dfrac{V_f^2-v_{y,k}^2}{2a_{\max}}}{V_f}, & \text{if } L_{y,k}>\dfrac{V_f^2-v_{y,k}^2}{2a_{\max}}\\ \dfrac{\sqrt{2a_{\max}L_{y,k}+{v_{y,k}}^2}-v_{y,k}}{a_{\max}}, & \text{otherwise}\end{cases} \quad (25)$$

For platoons in the same lane, the arrival time of the following platoon should satisfy the constraint as given by

$$t_{y,k}^{a}\geq t_{y,k-1}^{a}+t_{y,k-1}^{c}+T_s^{c} \ \forall y \text{ and } k>1 \quad (26)$$

where $t_{y,k-1}^{a}$ is the arrival time of the preceding platoon *k-1*. $t_{y,k-1}^{c}$ is the clearance time of the preceding platoon *k-1*. T_s^{c} is the safe time headway of the CAV. $v_{y,k}$ is the speed of the first vehicle in the k^{th} platoon in lane y at time t_c. $a_{\max}$ is the maximum comfortable acceleration. $L_{y,k}$ is the distance from the first vehicle of the k^{th} platoon in lane y to the stop line.

I. Platoon departure time constraints

Equation (27) indicates that the platoon should pass the intersection after the green start time of the phase selected. In addition, the departure time of the moving platoon should be equal to the arrival time in order to ensure that the moving platoon passes the intersection without stopping as given by (28).

$$t_{y,k}^{L}\geq t_{j,i}-M\left(1-\theta_{y,k,j}\right) \ \forall y,k,j,i \quad (27)$$

$$t_{y,k}^{L}=t_{y,k}^{a} \ \forall(y,k)\in\Gamma_m \quad (28)$$

V. Platoon Trajectory Planning

After deriving the signal timing scheme and arrival time of each platoon, the next step is to plan the trajectory of the first vehicle (CAV) in the platoon such that it can arrive at the planned arrival time. We consider that the CAV first accelerates to the desired speed with the maximum comfortable acceleration, and then drive to the stop line at the desired speed. This process can be described as

$$\frac{v_{y,k}^{e}-v_{y,k}}{a_{\max}}+\frac{L_{y,k}-\dfrac{{v_{y,k}^{e}}^2-{v_{y,k}}^2}{2a_{\max}}}{v_{y,k}^{e}}=t_{y,k}^{a}-t_c \quad (29)$$

$$0\leq v_{y,k}^{e}\leq v_{\max} \quad (30)$$

where $v_{y,k}^{e}$ is the desired speed of the first vehicle (CAV) in the k^{th} platoon in lane y.

It is worth noting that the number of HDVs in the platoon cannot be accurately estimated when the CAV penetration rate is very low (e.g., only one CAV is traveling in a group of moving HDVs). This has impacts on the CAV who may not follow the planned trajectory perfectly. In addition, the stochastic behavior of HDVs could also influence the behavior of CAVs. Therefore, the actual acceleration is then taken as the minimum of the acceleration calculated by the car-following model and planned acceleration, as given by (31). If the platoon does not follow the planned acceleration, the platoon trajectory is re-planned in order to ensure that the platoon reaches the stop line at the planned arrival time.

$$a^{c}=\min(a^{f},a^{m}) \quad (31)$$

where a^{c} is the actual acceleration. a^{f} is the acceleration calculated by the car-following model (e.g., ACC). a^{m} is the planned acceleration.

VI. Numerical Example

A. Experiment setup

To evaluate the proposed method, we choose a typical four-arm intersection. Each arm is set up with the dedicated left-turn, straight and right-turn lanes. The length of each lane is 560m, and the width of each lane is 3.5m. The communication zone is set as 300m of the intersection. Besides, the influence of the non-motorized vehicles and pedestrians is not considered.

In our simulation experiment, the Intelligent Driver Model (IDM) developed by Treiber [26] is applied to describe the car-following behavior of HDVs and the model parameters are set according to [26]. The motion of CAVs is controlled by the Adaptive Cruise Control (ACC) model whose parameters are calibrated based on real vehicle trajectory data by PATH Labs [27]. According to the assumptions made in Section 4.1, vehicles are generated based on the Poisson distribution. Each vehicle in the simulation environment is given a random number between 0 and 1. When the random number is less than the given penetration rate, it indicates that the vehicle is a CAV; Otherwise, this vehicle is a HDV. For each simulation run, the total simulation time is set as 3600s with a warm-up period of 10 minutes. The free-flow speed and maximum comfortable acceleration are set as 11.11 m/s and 2 m/s^2, respectively.

The simulation environment is constructed based on SUMO [28]. Traffic information including the vehicle type, location, speed and acceleration can be obtained through Traci, which is the traffic control interface of SUMO. The CAVs and signals in the simulation are also controlled by Traci. Gurobi 9.1.2 is applied to solve the optimization model. The upper limit of the solution time is set as 1s, and if the upper limit of the solution time is reached, the feasible solution solved by the solver is accepted. All simulation experiments are conducted on a computer with an Intel 2.81 GHz CPU and 16 GB memory.

B. Results

To demonstrate the effectiveness of the proposed model, we compare the results with those from the vehicle-actuated control model. In the vehicle-actuated control model, the minimum green duration and unit green extension time are set as 12 s and 3 s, respectively. The detector position is set as 24 m from the stop line, and the maximum green duration is set as 60 s. To avoid the effect of random factors, each case is repeated ten times.

TABLE I. AVERAGE DELAY UNDER CAV PENETRATION RATE OF 0.6

Demand (v/c)	Average Delay (s / veh)		
	Actuated Control	The proposed method	Decrease (%)
0.5	23.31	22.34	4.16
0.6	33.49	31.72	5.20
0.7	47.48	42.82	9.81
0.8	72.79	61.32	15.76
0.9	92.09	73.21	20.50
1.0	103.75	88.35	14.84
1.1	111.03	95.62	13.88

TABLE II. AVERAGE FUEL CONSUMPTION UNDER CAV PENETRATION RATE OF 0.6

Demand (v/c)	Average Fuel Consumption (ml / veh)		
	Actuated Control	The proposed method	Decrease (%)
0.5	56.92	54.61	4.06
0.6	63.77	60.33	4.50
0.7	65.21	61.10	6.31
0.8	76.31	68.51	10.22
0.9	78.74	70.51	13.07
1.0	82.09	74.25	9.55
1.1	84.65	79.04	6.63

Tables I and II show the average delay and average fuel consumptions under different degree of saturation with the CAV penetration rate of 0.6, respectively. It can be clearly observed that the proposed method exhibits better performance than that of the vehicle-actuated control method. The percentage reduction of the average delay increases with the increase of the degree of saturation (from 0.5 to 0.9) up to 20.5%. When the degree of saturation is higher than 0.9 (near saturation or oversaturation), the percentage reduction of the average delay decreases with the increase of the degree of saturation (>0.9). This could be because the number of vehicles in a platoon under the higher degree of saturation (e.g., >0.9) is larger than that under the lower degree of saturation (e.g., <0.9). In this case, the required green time is longer in order to accommodate a platoon to pass through the intersection completely, resulting in a longer cycle time and thus the increase of the delay. Similar results can be observed for the average fuel consumption as indicated in Table II.

Figs.8 and 9 show the average delay as a function of the CAV penetration rate when the degrees of saturation are 0.6 and 1, respectively. We can observe that the average delay decreases with the increase of the CAV penetration rate both for the undersaturated and saturated conditions. Compared with the average delay based on the vehicle-actuated control method, the percentage reduction of the delay of the proposed model increases substantially when the CAV penetration rate increases from 0.2 to 1 under the saturated condition as can be seen from Figs. 8(b) and 9(b). It is worth noting that when the CAV penetration rate is low (e.g., 0.2) in the undersaturated condition (v/c = 0.6), the proposed model performs even worse than the vehicle-actuated control model. This is due to the fact that the small proportion of CAVs (e.g., ≤ 20%) in the mixed traffic stream could result in large errors in platoon identification and estimation, leading to inefficient signal optimization.

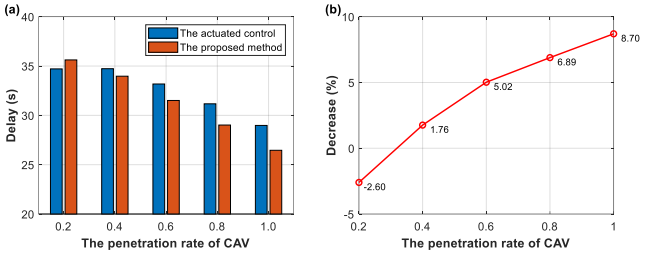

Figure 8. Average delay with different penetration rates for a saturation of 0.6.

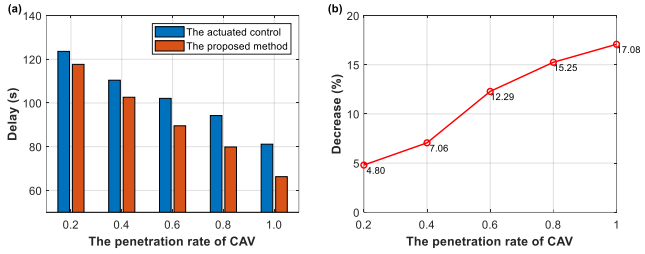

Figure 9. Average delay with different penetration rates for a saturation of 1.

VII. CONCLUSION

This study presents a bi-level integrated optimization method for traffic signals and vehicle trajectories in mixed traffic with CAVs and HDVs. The vehicles are divided into multiple platoons as the basic units for optimal control. The upper level is a MILP model that optimizes the signal timing scheme and the arrival time of each platoon at the stop line. The lower level optimizes the CAV trajectories based on the arrival times planned in the upper level to avoid stopping at the stop line. The simulation experiment is conducted to verify the effectiveness of the proposed method compared to the vehicle-actuated control method. The results show that the benefits of the proposed method over the vehicle-actuated control method increase with the traffic demand in the

undersaturated conditions (e.g., v/c<1). In particular, when the degree of saturation is 0.9, the percentage reductions of delay and fuel consumption are over 20% and 13%, respectively. When the intersection is saturated or oversaturated, the benefits of the proposed model decrease as the traffic demand increases, but still outperforms the vehicle-actuated control method. In addition, the benefits from the proposed model increases significantly with the increase of the CAV penetration rate.

This study reveals the great potential of the platoon-based integrated optimization of the traffic signal and vehicle trajectories. In future, we intend to extend the proposed method in two aspects. First of all, this study focuses on the longitudinal control of CAVs and no lane changes is allowed within the communication zone. Our future research could consider the lane change behavior of HDVs and the lateral control of CAVs. Secondly, this paper focuses on the integrated optimization of the CAVs and traffic signal of a single intersection, which can be further extended to consider multiple intersections.

REFERENCES

[1] B. Asadi and A. Vahidi, "Predictive Cruise Control: Utilizing Upcoming Traffic Signal Information for Improving Fuel Economy and Reducing Trip Time," IEEE Transactions on Control Systems Technology, vol. 19, no. 3, pp. 707-714, 2011.

[2] H. Yang, H. Rakha, and M. V. Ala, "Eco-Cooperative Adaptive Cruise Control at Signalized Intersections Considering Queue Effects," IEEE Transactions on Intelligent Transportation Systems, vol. 18, no. 6, pp. 1575-1585, 2017.

[3] S. E. Li, S. Xu, X. Huang, B. Cheng, and H. Peng, "Eco-Departure of Connected Vehicles With V2X Communication at Signalized Intersections," IEEE Transactions on Vehicular Technology, vol. 64, no. 12, pp. 5439-5449, 2015.

[4] M. Liu, S. Hoogendoorn, and M. Wang, "Receding Horizon Cooperative Platoon Trajectory Planning on Corridors with Dynamic Traffic Signal," Transportation Research Record, vol. 2674, no. 12, pp. 324-338, 2020/12/01 2020.

[5] B. HomChaudhuri, A. Vahidi, and P. Pisu, "Fast Model Predictive Control-Based Fuel Efficient Control Strategy for a Group of Connected Vehicles in Urban Road Conditions," IEEE Transactions on Control Systems Technology, vol. 25, no. 2, pp. 760-767, 2017.

[6] V. Milanes, J. Perez, E. Onieva, and C. Gonzalez, "Controller for Urban Intersections Based on Wireless Communications and Fuzzy Logic," IEEE Transactions on Intelligent Transportation Systems, vol. 11, no. 1, pp. 243-248, 2010.

[7] M. Liu, J. Zhao, S. Hoogendoorn, and M. Wang, "A single-layer approach for joint optimization of traffic signals and cooperative vehicle trajectories at isolated intersections," Transportation Research Part C: Emerging Technologies, vol. 134, p. 103459, 2022/01/01/ 2022.

[8] Q. Guo, L. Li, and X. Ban, "Urban traffic signal control with connected and automated vehicles: A survey," Transportation Research Part C: Emerging Technologies, vol. 101, pp. 313-334, Apr 2019.

[9] Z. Li, L. Elefteriadou, and S. Ranka, "Signal control optimization for automated vehicles at isolated signalized intersections," Transportation Research Part C: Emerging Technologies, vol. 49, pp. 1-18, 2014/12/01/ 2014.

[10] B. Xu et al., "Cooperative Method of Traffic Signal Optimization and Speed Control of Connected Vehicles at Isolated Intersections," IEEE Transactions on Intelligent Transportation Systems, vol. 20, no. 4, pp. 1390-1403, Apr 2019.

[11] Y. Feng, C. Yu, and H. X. Liu, "Spatiotemporal intersection control in a connected and automated vehicle environment," Transportation Research Part C: Emerging Technologies, vol. 89, pp. 364-383, Apr 2018.

[12] M. Q. Liu, J. Zhao, S. P. Hoogendoorn, and M. Wang, "An optimal control approach of integrating traffic signals and cooperative vehicle trajectories at intersections," Transportmetrica B:Transport Dynamics, Oct 22 2021.

[13] C. Chen, J. Wang, Q. Xu, J. Wang, and K. Li, "Mixed platoon control of automated and human-driven vehicles at a signalized intersection: Dynamical analysis and optimal control," Transportation Research Part C: Emerging Technologies, vol. 127, p. 103138, 2021/06/01/ 2021.

[14] Y. Feng, K. L. Head, S. Khoshmagham, and M. Zamanipour, "A real-time adaptive signal control in a connected vehicle environment," Transportation Research Part C: Emerging Technologies, vol. 55, pp. 460-473, 2015/06/01/ 2015.

[15] N. J. Goodall, B. L. Smith, and B. Park, "Traffic Signal Control with Connected Vehicles," Transportation Research Record, no. 2381, pp. 65-72, 2013.

[16] C. Priemer and B. Friedrich, "A decentralized adaptive traffic signal control using V2I communication data," in 2009 12th International IEEE Conference on Intelligent Transportation Systems, 2009, pp. 1-6.

[17] J. Lee, B. Park, and I. Yun, "Cumulative Travel-Time Responsive Real-Time Intersection Control Algorithm in the Connected Vehicle Environment," Journal of Transportation Engineering, vol. 139, no. 10, pp. 1020-1029, Oct 1 2013.

[18] Y. Guo, J. Ma, C. Xiong, X. Li, F. Zhou, and W. Hao, "Joint optimization of vehicle trajectories and intersection controllers with connected automated vehicles: Combined dynamic programming and shooting heuristic approach," Transportation Research Part C: Emerging Technologies, vol. 98, pp. 54-72, Jan 2019.

[19] S. Chen and D. Sun, "An Improved Adaptive Signal Control Method for Isolated Signalized Intersection Based on Dynamic Programming," IEEE Intelligent Transportation Systems Magazine, vol. 8, no. 4, pp. 4-14, Win 2016.

[20] B. Beak, K. L. Head, and Y. H. Feng, "Adaptive Coordination Based on Connected Vehicle Technology," Transportation Research Record, no. 2619, pp. 1-12, 2017.

[21] W. Li and X. Ban, "Connected Vehicles Based Traffic Signal Timing Optimization," IEEE Transactions on Intelligent Transportation Systems, vol. 20, no. 12, pp. 4354-4366, Dec 2019.

[22] C. H. Yu, Y. H. Feng, H. X. Liu, W. J. Ma, and X. G. Yang, "Integrated optimization of traffic signals and vehicle trajectories at isolated urban intersections," Transportation Research Part B: Methodological, vol. 112, pp. 89-112, Jun 2018.

[23] C. Yu, Y. Feng, H. X. Liu, W. Ma, and X. Yang, "Integrated optimization of traffic signals and vehicle trajectories at isolated urban intersections," Transportation Research Part B: Methodological, vol. 112, pp. 89-112, Jun 2018.

[24] X. Liang, S. I. Guler, and V. V. Gayah, "Signal Timing Optimization with Connected Vehicle Technology: Platooning to Improve Computational Efficiency," Transportation Research Record, vol. 2672, no. 18, pp. 81-92, Dec 2018.

[25] Q. He, K. L. Head, and J. Ding, "PAMSCOD: Platoon-based arterial multi-modal signal control with online data," Transportation Research Part C: Emerging Technologies, vol. 20, no. 1, pp. 164-184, 2012/02/01/ 2012.

[26] M. Treiber, A. Hennecke, and D. Helbing, "Congested traffic states in empirical observations and microscopic simulations," Physical review E, vol. 62, no. 2, p. 1805, 2000.

[27] V. Milanés and S. E. Shladover, "Modeling cooperative and autonomous adaptive cruise control dynamic responses using experimental data," Transportation Research Part C: Emerging Technologies, vol. 48, pp. 285-300, 2014.

[28] P. A. Lopez et al., "Microscopic traffic simulation using sumo," in 2018 21st international conference on intelligent transportation systems (ITSC), 2018, pp. 2575-2582: IEEE.